SC_nS Linear Chain Production by Direct Laser Ablation

Andrei Burnin and Joseph J. BelBruno*

Dartmouth College, Department of Chemistry and Center for Nanomaterials Research, Hanover, New Hampshire 03755

Received: March 31, 2003; In Final Form: July 16, 2003

Cumulenic polycarbons SC_nS ($n = 2-27$) were generated by laser ablation of mixtures of elemental carbon and sulfur. The resulting molecules were analyzed in a time-of-flight mass spectrometer. The spectra exhibited ideal odd/even intensity alternation attributed to their relative stability and the formation mechanism of the clusters. The structures and energies of the neutral and charged carbon chains capped with two sulfur atoms were also studied by density functional theory. The computational results were consistent with the experimental observations. Evidence of sulfur poisoning of fullerene formation was observed and explained in terms of one of the existing models for fullerene formation and growth.

I. Introduction

Cumulenic polycarbons and polycarbons terminated by heteroatoms are of particular interest because of their involvement in the chemistry of the diffuse interstellar medium[1,2] as well as their extraordinary electrical properties.[3] XC_n and XC_nX chain-like molecules have been studied via interstellar band spectra, by means of computational chemistry, and have been synthesized and characterized in the laboratory.

In general, due to their high reactivity, bare carbon chains are readily terminated by a wide variety of atoms and groups of atoms.[4] Capping heteroelements have been reported to include B, Al, P, As, Bi,[5] Ge,[6] and, additionally, atoms of the transition metals: Ti, Zr, V, Cr, W, Fe, and Ni.[7] Recently, Ball et al. have reported cavity ring down spectroscopy detection of linear odd-numbered HC_nH molecules obtained by supersonic expansion of a dilute mixture of diacetylene in argon through a pulsed discharge nozzle.[8] It has also been shown that tangible amounts of NC_nN molecules could be produced[9,10] and used as reagents in organic synthesis.[11]

Group VIa elements are particularly efficient capping agents.[12−14] Small even- and odd-numbered polycarbon disulfides SC_nS ($n = 2-6$) were generated using electron impact ionization of 2*H*,5*H*,8*H*-benzo[1,2-*d*:3,4-*d*′:5,6-*d*″]tri(1,3-dithiol)-2,5,8-trion and studied by collisional activation.[15] Small ($n = 1-5$) asymmetric and symmetric carbon sulfur clusters have been produced in an argon matrix. For these clusters, absorption spectra were recorded and the chemical nature of the absorbing species was identified using computed frequencies of structurally optimized linear clusters.[16] Longer chain SC_nS^+ and SC_nS^- clusters were generated and detected in a TOF mass spectrometer.[17]

Typically in cluster experiments, spectroscopic identification is combined with a computational approach. Thus, there have been previous theoretical reports of the properties of such molecules.[18,19] Recently, our group has described the results of a DFT study of long ($n \leq 16$) C_nS anionic and cationic clusters.[20] Continuing our previous work, here we report the results of a combined experimental and theoretical study of SC_nS clusters that include up to 27 carbon atoms.

II. Experimental Details

The polycarbon mono- and disulfide chains were generated in a time-of-flight mass spectrometer by laser ablation using a Nd:YAG laser (Spectra Physics DCR-11) operated at the fundamental (1064 nm) and the second (532 nm) harmonic in the Q-switched (∼7 ns pulse) regime with a repetition rate of 10 Hz. The laser beam was focused onto the target with a 50 cm focal length quartz lens to provide combined fluences of up to 4.5 J cm^{-2}. Various molar ratio mixtures of graphite (Alfa Aesar) and sulfur (Mallinckrodt) powders were employed as ablation targets. Targets of both packed pellets and gently pressed powder mixtures were employed. Mass spectra were independent of the sample preparation technique. Postgeneration, the clusters spatially spread toward the extraction and acceleration regions. Application of the extracting and accelerating high-voltage pulses, delayed by 55 or 80 ms, provided improved detection of smaller or larger species, respectively. At the exit of the acceleration region, all positively charged clusters have 750 eV kinetic energy and travel toward the detector through a 2.28 m field-free flight tube. Species of different masses are discriminated by their respective times-of-flight and detected by a Channeltron electron multiplier (Galileo Electro Optics). Signals from the detector are averaged over 2000 sweeps and processed in a PC. The base pressures in the ablation and detection regions were approximately 1×10^{-6} Torr. The working pressure in the ablation region was higher but never out of the 10^{-6} Torr range. The working pressure in the detection region was essentially unchanged.

For analysis of neutral clusters, an electron gun was employed to ionize the neutral species remaining in the plasma after a suitable delay that allowed plasma cooling. The electron gun was oriented to eject electrons in the direction perpendicular to the cluster flow as the ablated material exits the target region (Figure 1). To prevent deflection of the laser-produced positive clusters by the outer grid of the electron gun, the normal polarity of the system was reversed. The grid was grounded and a negative 50−200 V potential was applied to the electron gun

* To whom correspondence should be addressed. E-mail: jjbchem@dartmouth.edu.

10.1021/jp0304071 CCC: $25.00
Published on Web 10/17/2003

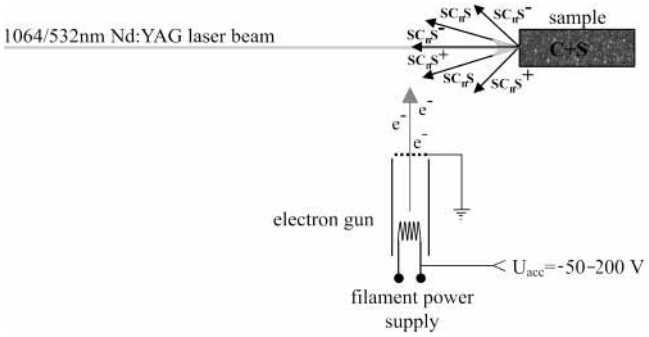

Figure 1. Electron gun-sample configuration. $\mathbf{U}_{acc}$ is the electron acceleration potential.

filament to provide the repulsive field needed to direct the electrons toward the clusters.

III. Theoretical Calculations

All DFT calculations, at the B3LYP level of theory with the 6-311G** basis set, were performed using the GAUSSIAN 98 suite of programs.[21] Single-point calculations at the same level of theory were performed at the optimized neutral cluster geometries in order to find vertical ionization energies and electron affinities of the neutral species. Adiabatic properties were obtained using optimized geometries to calculate total energies for both the ionic and neutral clusters.

IV. Results and Discussion

Experimental Results. Figure 2a and b presents TOF mass spectra obtained by direct laser vaporization, using the combined 1064 and 532 nm beams, of a 2:1 (carbon to sulfur) molar mixture with two different values of delay time. All spectra exhibit signals from three species of clusters: S_n^+, CS_n^+, and SC_nS^+. The mass peaks corresponding to 160 and 256 amu have the largest intensities because they represent the sum of two contributions to the overall signal: $C_8S_2^+$ plus S_5^+ and $C_{16}S_2^+$ plus S_8^+, respectively. The sulfur magic numbers, 5 and 8 for both positive and neutral sulfur clusters, are well-known from experiment and theory.[22,23] Apart from the double-contribution case, the signals from the mono- and disulfides exhibit alternating intensities arising from the odd- and even-carbon clusters. Unless otherwise noted, these signals result from direct production of ions in the plasma by laser irradiation.

C_nS^+. In the spectrum obtained at a delay time of 55 μs (Figure 2a), the three peaks from C_3S^+, C_4S^+, and C_5S^+ represent the only mass peaks from this family of clusters. Among the three, the C_4S^+ mass peak is approximately four times less intense than its neighboring family members. Commonly, such an intensity alternation is assumed to be indicative of the relative abundance of the corresponding species from the ablated material in the microplasma and, therefore, of the relative stability.[16,18] In keeping with this interpretation, we conclude that the odd-carbon molecular ions of this series are favored.

SC_nS^+. The intensity alternation for disulfides is opposite that observed for the monosulfides (Figure 2a and b). In the mass spectrum, clusters with an even number of carbon atoms demonstrate larger intensities than their odd-numbered neighbors. We have carried out a complementary experiment to study the abundances of neutral clusters in the cloud traveling from the source toward the extraction region. Soft electron impact ionization, 50−200 eV, of neutral species allowed us to probe the distribution of these clusters. Even-carbon peak intensities in the time-of-flight mass spectra rapidly increase as the voltage is increased from 50 V, but the peak intensities plateau very quickly. Peak ratios then remain unchanged as the electron energy is further increased to 200 V. Above 200 V, the field from the electron gun distorts the TOF spectrum. Comparing the two mass spectra in parts b and c of Figure 2, one can observe the net change in the relative intensities due to the ionization of neutral clusters. The overall intensity pattern is visibly altered in Figure 2c, with the intensities of peaks corresponding to clusters having $n + 1$ (n is any even value from 2 to 10) increasing significantly from the corresponding intensities in Figure 2a and b.

An interesting observation from any of the spectra shown in Figure 2 relates to the formation of fullerenes. In our apparatus, during the ablation of pure carbon, we observe strong signals from C_{60} and C_{70} at 160 and 173 μs TOF, respectively, as well as signals from other fullerenes C_n, where $n = 34-120$ ($\Delta n = 2$). The mass spectra of graphite mixed with sulfur exhibit no fullerene signal at any flight time; see for example Figure 2b. Fullerene formation is completely poisoned in the presence of sulfur.

Computational Results. In the computational portion of this work, we have determined the optimized geometries and energies of SC_nS neutral clusters as well as the corresponding anionic and cationic forms. The electronic ground state of the neutral clusters with an even number of carbon atoms is $^3\Sigma$, and for those with an odd number of carbon atoms, it is $^1\Sigma$. All charged forms have a $^2\Pi$ electronic ground state. Here, we report the bond lengths, Mulliken charge distributions, and atomization energies of only the neutral SC_nS clusters up to $n = 18$ (Table 1). (Data for the optimized geometries of the positively and negatively charged forms of polycarbon disulfides are available directly from the authors.) The sulfur−carbon bond length is in the range 1.560−1.570 Å and is consistent with the accepted sulfur−carbon double-bond length. The carbon−carbon bond lies in the 1.272−1.286 Å range, indicating cumulenic behavior, which is more pronounced in odd-numbered clusters. As in the case of the C_nS clusters,[20] sulfur atoms carry the positive charge, whereas the negative charge is distributed along the chain of carbon atoms for those clusters with seven or fewer carbon atoms. Larger clusters include carbon atoms that also carry positive charge. Since the clusters are symmetric, the molecules do not have a permanent dipole moment. The only available comparison point for the calculated atomization energies is the published value[24] for CS_2. Our calculated result, 11.71 eV, is in excellent agreement with the accepted value, 11.73 eV.

For the SC_nS^+ clusters, the carbon−sulfur bond length is in the range of 1.546−1.559 Å, shorter than that in the corresponding neutral clusters. The carbon chain length (cluster length minus the distance of the carbon−sulfur bonds), however, is slightly elongated in small clusters and approximately unchanged in longer molecules. The SC_nS^- clusters exhibit longer carbon−sulfur bonds in comparison to those of the neutral clusters, 1.595−1.644 Å, while the carbon chain length is increased over those of the neutral molecules. The behavior of the carbon−sulfur bond lengths and carbon chain lengths as a function of net cluster charge may be understood with the help of the relevant molecular orbitals (Figure 3). Because the even-numbered neutral clusters have a triplet ground state, the HOMO must be considered both for ionization and electron addition. The antibonding character (of what is nominally a nonbonding component) between the carbon and sulfur atoms in the overall bonding HOMO (Figure 3a) explains the bond elongation when an electron is added to the neutral cluster and the bond

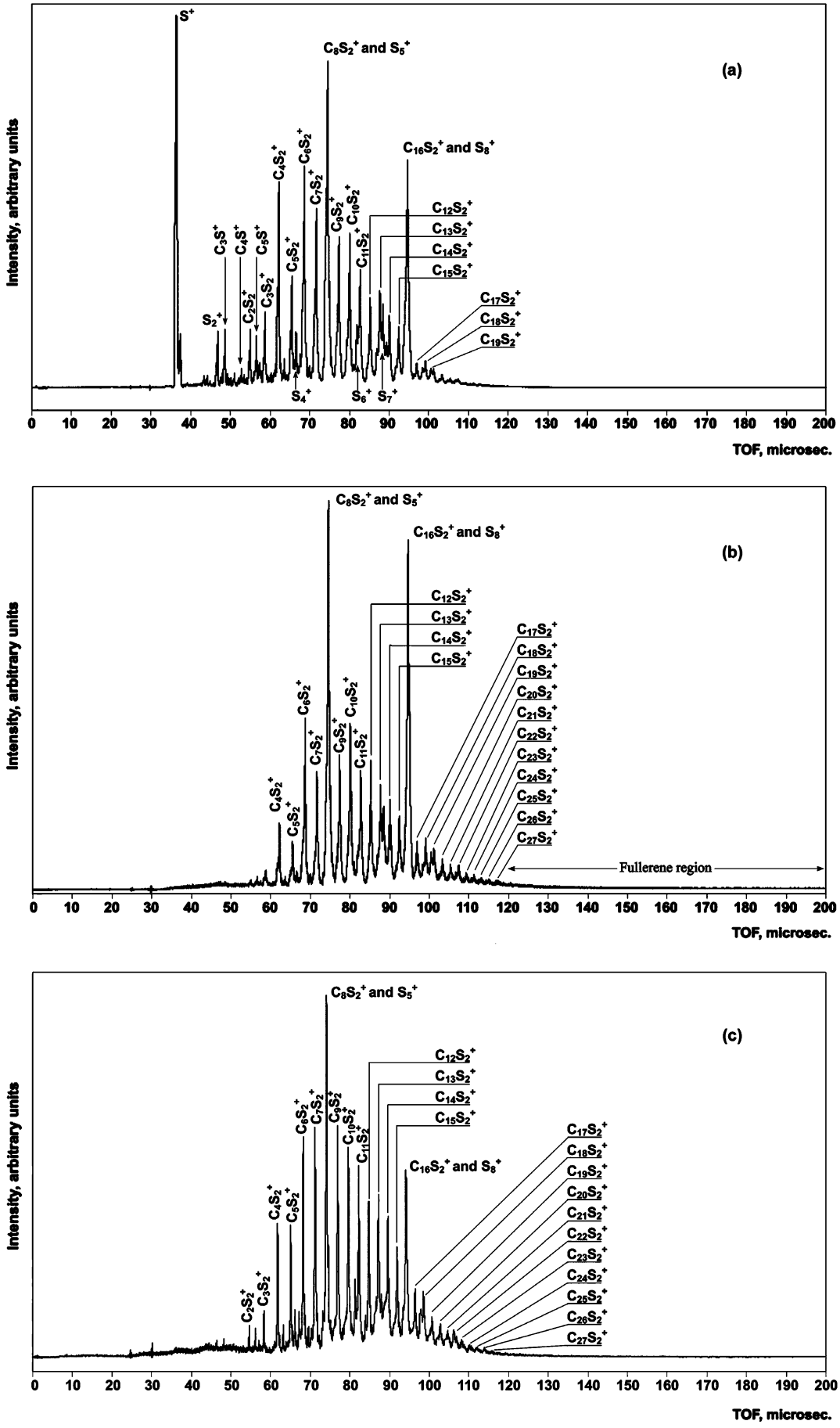

Figure 2. Mass spectra of the 2:1 mixture of carbon and sulfur powder at delay times of 55 μs (a), 80 μs (b), and 80 μs with the electron gun (c).

TABLE 1: Optimized Geometry and Mulliken Charge Distribution for Neutral SC_nS Clusters

n	Bond length, Å / SC_nS / Mulliken charge	Atomization energy, eV
1	1.560 1.560 S—C—S 0.11 -0.21 0.11	11.71
2	1.580 1.273 1.580 S—C—C—S 0.14 -0.14 -0.14 0.14	16.77
3	1.563 1.274 1.274 1.563 S—C—C—C—S 0.14 -0.13 -0.01 -0.13 0.14	24.11
4	1.575 1.272 1.286 1.272 1.575 S—C—C—C—C—S 0.16 -0.13 -0.03 -0.03 -0.13 0.16	29.60
5	1.565 1.273 1.275 1.275 1.273 1.565 S—C—C—C—C—C—S 0.16 -0.03 -0.11 -0.04 -0.11 -0.03 0.16	36.66
6	1.573 1.272 1.283 1.272 1.283 1.272 1.573 S—C—C—C—C—C—C—S 0.18 -0.02 -0.07 -0.09 -0.09 -0.07 -0.02 0.18	42.36
7	1.566 1.273 1.277 1.275 1.275 1.277 1.273 1.566 S—C—C—C—C—C—C—C—S 0.17 0.05 -0.14 -0.04 -0.08 -0.04 -0.14 0.05 0.17	49.25
8	1.572 1.273 1.282 1.273 1.281 1.273 1.282 1.273 1.572 S—C—C—C—C—C—C—C—C—S 0.18 0.05 -0.12 -0.18 0.07 0.07 -0.18 -0.12 0.05 0.18	55.08
9	1.567 1.273 1.278 1.274 1.276 1.276 1.274 1.278 1.273 1.567 S—C—C—C—C—C—C—C—C—C—S 0.17 0.08 -0.18 -0.17 -0.06 0.32 -0.06 -0.17 -0.18 0.08 0.17	61.85
10	1.571 1.273 1.281 1.273 1.280 1.274 1.280 1.273 1.281 1.273 1.571 S—C—C—C—C—C—C—C—C—C—C—S 0.17 -0.07 -0.01 0.11 -0.19 -0.02 -0.02 -0.19 0.11 -0.01 -0.07 0.17	67.78
11	1.567 1.273 1.278 1.274 1.277 1.276 1.276 1.277 1.274 1.278 1.273 1.567 S—C—C—C—C—C—C—C—C—C—C—C—S 0.16 -0.02 -0.09 0.16 -0.05 -0.35 0.38 -0.35 -0.05 0.16 -0.09 -0.02 0.16	74.48
12	1.571 1.273 1.281 1.273 1.280 1.274 1.280 1.274 1.280 1.273 1.281 1.273 1.571 S—C—C—C—C—C—C—C—C—C—C—C—C—S 0.17 -0.04 -0.05 0.17 -0.09 -0.30 0.15 0.15 -0.30 -0.09 0.17 -0.05 -0.04 0.17	80.47
13	1.567 1.273 1.278 1.274 1.277 1.275 1.276 1.276 1.275 1.277 1.274 1.278 1.273 1.567 S—C—C—C—C—C—C—C—C—C—C—C—C—C—S 0.17 -0.01 -0.10 0.11 0.08 -0.20 -0.30 0.50 -0.30 -0.20 0.08 0.11 -0.10 -0.01 0.17	87.11
14	1.570 1.273 1.281 1.273 1.279 1.274 1.279 1.274 1.279 1.274 1.279 1.273 1.281 1.273 1.570 S—C—C—C—C—C—C—C—C—C—C—C—C—C—S 0.17 0.01 -0.10 -0.03 0.22 -0.12 -0.32 0.17 0.17 -0.32 -0.12 0.22 -0.03 -0.10 0.01 0.17	93.16
15	1.568 1.273 1.279 1.274 1.277 1.275 1.276 1.276 1.276 1.276 1.275 1.277 1.274 1.279 1.273 1.568 S—C—C—C—C—C—C—C—C—C—C—C—C—C—C—C—S 0.17 0.03 -0.13 -0.03 0.08 0.23 -0.34 -0.21 0.40 -0.21 -0.34 0.23 0.08 -0.03 -0.13 0.03 0.17	99.75
16	1.570 1.273 1.280 1.273 1.279 1.274 1.279 1.275 1.279 1.275 1.279 1.274 1.279 1.273 1.280 1.273 1.570 S—C—C—C—C—C—C—C—C—C—C—C—C—C—C—C—C—C—S 0.17 0.04 -0.12 -0.10 0.04 0.34 -0.21 -0.32 0.16 0.16 -0.32 -0.21 0.34 0.04 -0.10 -0.12 0.04 0.17	105.84
17	1.568 1.273 1.279 1.274 1.277 1.275 1.277 1.276 1.276 1.276 1.276 1.277 1.275 1.277 1.274 1.279 1.273 1.568 S—C—C—C—C—C—C—C—C—C—C—C—C—C—C—C—C—C—C—S 0.17 0.06 -0.15 -0.10 -0.02 0.32 0.05 -0.29 -0.29 0.48 -0.29 -0.29 0.05 0.32 -0.02 -0.10 -0.15 0.06 0.17	112.39
18	1.570 1.273 1.280 1.273 1.279 1.274 1.279 1.275 1.279 1.275 1.279 1.275 1.279 1.274 1.279 1.273 1.280 1.273 1.570 S—C—C—C—C—C—C—C—C—C—C—C—C—C—C—C—C—C—C—C—S 0.17 0.06 -0.14 -0.16 0.02 0.21 0.26 -0.24 -0.34 0.16 0.16 -0.34 -0.24 0.26 0.21 0.02 -0.16 -0.14 0.06 0.17	118.52

TABLE 2: Incremental Atomization Energies, Ionization Energies, and Electron Affinities for SC_nS Clusters

SC_nS	incremental atomization energy, eV			ionization energy, eV		electron affinity, eV	
n	neutral	cation	anion	adiabatic IE	vertical IE	adiabatic EA	vertical EA
1				10.13	10.13	0.14	−0.04
2	5.06	6.55	7.19	8.64	8.79	2.26	2.09
3	7.34	6.87	6.41	9.11	9.14	1.33	1.18
4	5.48	6.49	6.87	8.11	8.27	2.71	2.54
5	7.06	6.68	6.38	8.49	8.53	2.03	1.91
6	5.70	6.45	6.69	7.74	7.90	3.03	2.86
7	6.89	6.57	6.36	8.06	8.11	2.50	2.39
8	5.83	6.42	6.60	7.47	7.63	3.27	3.11
9	6.78	6.51	6.35	7.74	7.79	2.84	2.74
10	5.93	6.41	6.54	7.26	7.41	3.46	3.30
11	6.70	6.47	6.34	7.49	7.54	3.10	3.01
12	6.00	6.40	6.51	7.09	7.24	3.61	3.46
13	6.64	6.44	6.33	7.29	7.34	3.31	3.22
14	6.05	6.39	6.48	6.95	7.10	3.74	3.59
15	6.59	6.42	6.32	7.12	7.17	3.48	3.40
16	6.09	6.39	6.47	6.83	6.98	3.85	3.70
17	6.55	6.40	6.32	6.98	7.02	3.62	3.54
18	6.13	6.38	6.46	6.72	6.87	3.95	3.80

shortening when a cation is formed. The electron is added into or removed from this orbital in which the sulfur atomic orbital with nonbonding electrons plays a major role. In the case of the odd-numbered neutral clusters, which are singlets, the

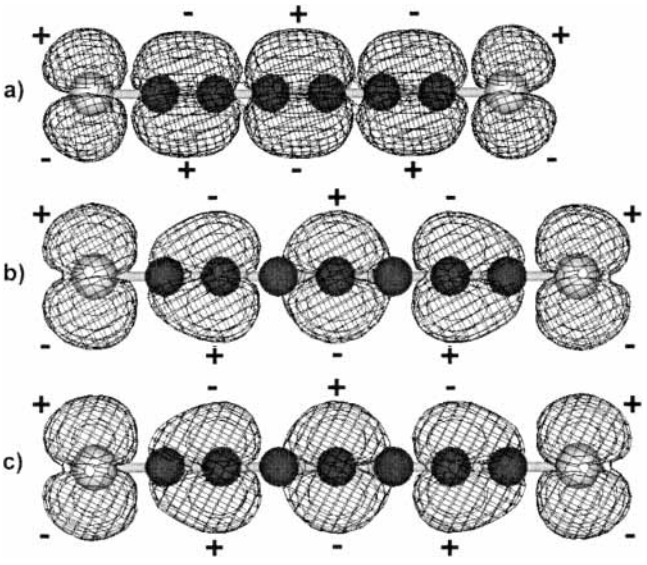

Figure 3. (a) HOMO-α orbital of the SC_6S cluster; (b) HOMO-α orbital of the SC_7S cluster; (c) LUMO-α orbital of the SC_7S cluster. The orbitals populated with β spins lie along the same chain axis but are in the plane perpendicular to that of the α-orbitals. These two clusters are representative of the even- and odd-carbon clusters, respectively.

LUMO must be examined in the formation of the anion and the HOMO for the ionization process. Both the HOMO and the LUMO have antibonding character along the carbon−sulfur bond, as described for the even-numbered clusters (Figure 3b and c), and thus, the same behavior with respect to electron addition or ionization is expected of the carbon−sulfur bond in the odd-numbered clusters as in the even-numbered ones. The sulfur atomic orbital contribution to both the HOMO and LUMO is very large.

Single-point energy calculations for the positively and negatively charged species, at the optimized geometry of the neutral clusters, were performed to compute vertical ionization energies and electron affinities for all SC_nS clusters. The corresponding adiabatic values were obtained as the differences between the energies of optimized, or relaxed, charged and neutral structures. The electron affinities, as usual, are reported as the negative of the energy change that occurs for the $SC_nS + e^- \rightarrow SC_nS^-$ vertical and adiabatic processes. The electron affinities of even-numbered clusters are energetically lower because the addition of an electron to the π-orbital having two unpaired electrons is more favorable than placing an electron in the next highest energy vacant orbital, as is required for the odd carbon clusters. The negative vertical electron affinity for the SCS cluster indicates that its anion is not stable. The summarized data, including incremental atomization energies, ionization energies, and electron affinities, are presented in Table 2. Incremental atomization energies were calculated in the standard fashion from the atomization energy differences, $\Delta E(SC_nS) = E(SC_nS) - E(SC_{n-1}S)$, for ions and neutrals. Figure 4 graphically shows how these properties vary with the number of carbon atoms.

The formation of the doubly sulfur terminated carbon chains appears to be a favored process. If one assumes that the monosulfide chains are formed rapidly, the termination of the chain growth by the addition of a second sulfur atom may be a controlling process in the yields of the respective ions. The capping of the monosulfide clusters, C_nS and C_nS^+, after carbon chain propagation could result from any of three different processes:

$$SC_n + S \rightarrow SC_nS \quad (1)$$

$$SC_n^+ + S \rightarrow SC_nS^+ \quad (2)$$

$$SC_n + S^+ \rightarrow SC_nS^+ \quad (3)$$

The three reaction channels were treated computationally. These calculations employed the energies of the C_nS reactants from our previous work.[20] Reaction energies for the three possible channels for the chain termination were determined, as shown in Figure 5.

Discussion. In our previous theoretical work,[20] we have computed the properties of optimized linear C_nS and C_nS^+ clusters. The calculated ground-state incremental atomization energies of the positive and neutral clusters with an even number of carbon atoms were shown to be lower than the atomization energies of those with an odd number of carbon atoms. The latter were characterized as more stable, in agreement with the experiments for C_nS and C_nS^+ reported here.

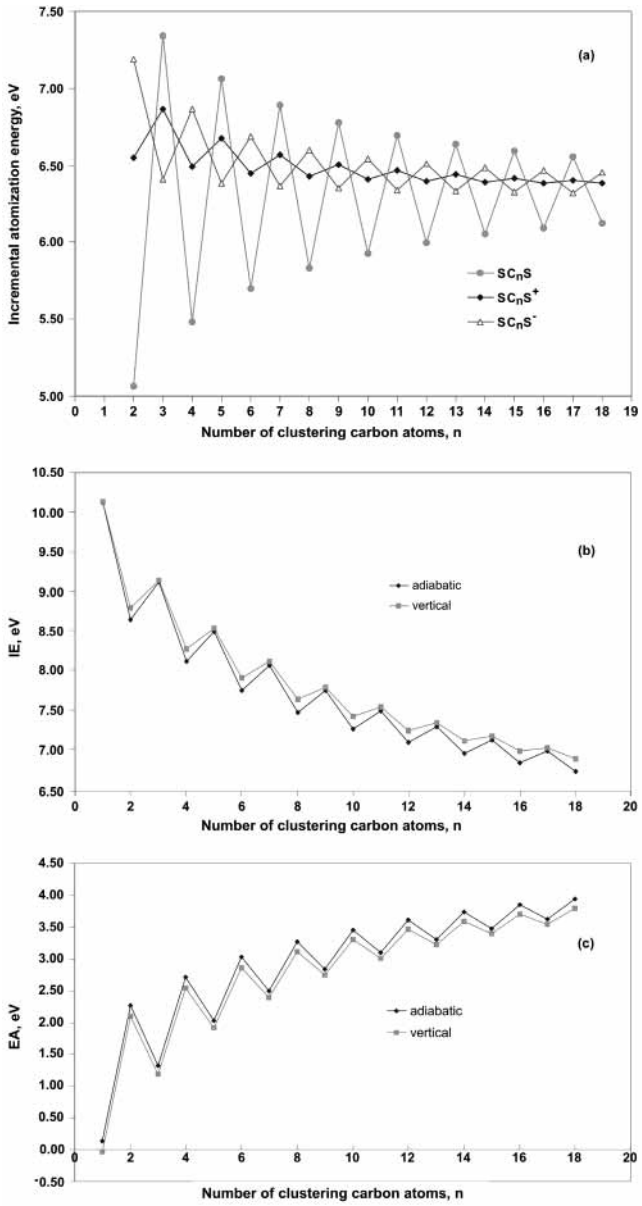

Figure 4. Incremental atomization energies (a), ionization energies (b), and electron affinities (c) of SC_nS clusters versus number of clustering carbon atoms *n*.

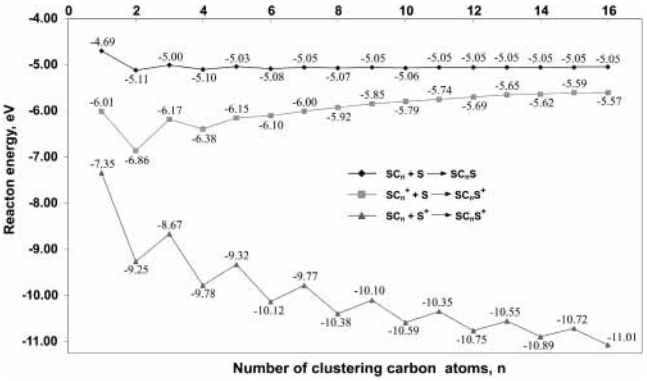

Figure 5. Energies of the possible chain termination reactions.

In the experiments discussed above, the even-numbered SC_nS^+ clusters exhibited higher intensities than the odd-carbon clusters for direct ion formation within the plasma. This observation does not agree with the computational results for stability based on the incremental atomization energy point of view (Table 2). Since the thermodynamics do not appear to control produce yield, one must look to kinetic factors. We may consider two of the possible channels, reactions 2 and 3, for sulfur capping leading to the formation of a cation in the ablated sample. The reaction energies for reaction 2, when $n \geq 4$, are nearly independent of the number of carbon atoms, as shown in Figure 5. Thus, this capping mechanism cannot be the source of the observed even−odd alternation. In contrast, the energy for reaction 3 strongly alternates from even to odd numbers of clustering carbon atoms, favoring the even carbon clusters. This is consistent with the experimental results. In addition, reaction 3 requires the presence of S^+ in the plasma, which seems to be abundant in the laser-ablated vapor, as shown in the mass spectrum in Figure 2a. Thus, we conclude that the relative abundances of SC_nS^+ clusters produced directly by laser irradiation appear to be kinetically controlled.

The use of soft electron ionization of the cooled plasma resulted in an increase in the apparent abundance of the odd clusters. The effect of electron impact ionization was observed by examining the differences in the spectra shown in Figure 2b and 2c. These changes in intensity result from the ionization of neutral clusters whose intensities are added to those of the cations produced directly by the laser. The neutral cluster abundances are not explained by kinetic factors, that is reactions 1−3, since the only applicable process, reaction 1, predicts yields for the ion intensities that would be energetically independent of the number of carbon atoms in a chain. Instead, the odd−even alternation for neutral clusters results from energetically controlled processes that produce the odd-carbon clusters in greater yield. The spectral intensities of the neutrals are seen to agree with theoretical predictions based on the incremental atomization energies (Figure 4a); the physical basis is usually cited as the determining factor in such studies.[16,18]

The plots of vertical and adiabatic ionization energies of neutral SC_nS clusters versus the number of cluster carbon atoms (Figure 4b) indicate that the ionization process is energetically much less expensive for even-numbered clusters than for odd-numbered ones. This computational result is consistent with the experimental results from direct production of SC_nS^+ clusters as well as production of neutral clusters by electron impact. The difference in ionization energy for odd- and even-numbered clusters is predicted to be significant for smaller molecules, to decay as the chains lengthen, and to finally disappear for larger species. For laser production of the cations, a process with relatively low available energy, the magnitude of the ionization energy is an important variable and exerts a major influence on the ion distribution. For electron impact, the available energy is sufficiently large that the value of the ionization energy is no longer a controlling factor.

The poisoning of fullerene formation provides information relevant to the fullerene formation mechanism. According to a number of the existing models for fullerene formation,,[25−27] carbon chains ($n \leq 10$) play a crucial role in the growth initiation of fullerenes. As the chains become larger than 10 carbon atoms, cyclic clusters preferentially form.[28−30] The cyclization is impossible if one end of a carbon chain is terminated with sulfur, since the formation of cyclic carbon−sulfur clusters was computationally demonstrated in our previous work[20] to be energetically unfavorable. Thus, the termination of one end of a carbon chain by a sulfur atom prevents further aggregation toward large cyclic and polycyclic structures, instead stimulating further propagation of the chain to at least 27 carbon atoms, the limit of our experimental observations. Chain growth can be stopped by attachment of the second sulfur atom at any step.

V. Conclusion

We have successfully generated linear polycarbon mono- and disulfides with a chain length of up to 27 carbon atoms. The ions were analyzed in a time-of-flight mass spectrometer. The observed intensity alternation of SC_nS^+ mass peaks was opposite that predicted by incremental bonding calculations. This observation was explained from a kinetic point of view. Soft electron ionization was successfully used to estimate the abundances of the neutral clusters whose intensities were consistent with the incremental atomization energies or thermodynamic control. Properties of SC_nS clusters and their positively and negatively charged ions were calculated using a DFT approach at the B3LYP level of theory. The observed poisoning of fullerene formation was shown to be consistent with the general mechanism for the fullerene formation.

References and Notes

(1) Allamandola, L. J.; Hudgins, D. M.; Bauschicher, C. W., Jr.; Langhoff, S. R. *Astron. Astrophys* **1999**, *352*, 659.
(2) Saito, S. *Sulfur Rep.* **1999**, *21*, 401.
(3) Spiro, C. L.; Banholtzer, W. F.; McAtee, D. S. *Thin Solid Films* **1992**, *220*, 120.
(4) Hino, S.; Okada, Y.; Iwasaki, K. *Surf. Rev. Lett.* **2002**, *9*, 1263.
(5) Huang, R. B.; Wang, C. R.; Liu, Z. Y.; Zheng, L. S.; Qi, F.; Sheng, L. S.; Yu, S. Q.; Zhang, Y. W. *Z. Phys. D* **1995**, *33*, 49.
(6) Leleyter, M. *Z. Phys. D* **1991**, *20*, 81−83.
(7) Leleyter, M. *Z. Phys. D* **1991**, *20*, 85−87.
(8) Ball, C. D.; McCarthy, M. C.; Thaddeus, P. *J. Chem. Phys.* **2000**, *112*, 10149.
(9) Groesser, T.; Hirsch, A. *Angew. Chem.* **1993**, *105*, 1390.
(10) Schermann, G.; Grosser, T.; Hampel, F.; Hirsch, A. *Chem.—Eur. J.* **1997**, *3*, 1105.
(11) Schermann, G.; Vostrowsky, O.; Hirsch, A. *Eur. J. Org. Chem.* **1999**, 2491.
(12) Liu, Z. Y.; Huang, R. B.; Zheng, L. S. *Int. J. Mass Spectrom. Ion Process.* **1996**, *155*, 79.
(13) Wang, H.; Huang, R.; Chen, H.; Lin, M.; Zheng, L. *J. Phys. Chem. A* **2001**, *105*, 4653.
(14) Suelzle, D.; Beye, N.; Fanghaenel, E.; Schwarz, H. *Chem. Ber.* **1990**, *123*, 2069.
(15) Szczepanski, J.; Hoydyss, R.; Fuller, J.; Vala, M. *J. Phys. Chem. A* **1999**, *103*, 2975.
(16) Pascoli, G.; Lavendy, H. *Int. J. Mass Spectrom.* **2001**, *206*, 153.
(17) Liu, Z.; Tang, Z.; Huang, R.; Zhang, Q.; Zheng, L. *J. Phys. Chem. A* **1997**, *101*, 4019.
(18) Bosoon, L.; Sungyul, L. *Chem. Phys. Lett.* **1998**, *286*, 171.
(19) Pascoli, G.; Lavendy, H. *Int. J. Mass Spectrom. Ion Process.* **1998**, *181*, 135.
(20) Tang, Z.; BelBruno, J. J. *Int. J. Mass Spectrom.* **2001**, *208*, 7.
(21) Frisch, M. J.; Trucks, G. W.; Schlegel, H. B.; Scuseria, G. E.; Robb, M. A.; Cheeseman, J. R.; Zakrzewski, V. G.; Montgomery, J. A., Jr.; Stratmann, R. E.; Burant, J. C.; Dapprich, S.; Millam, J. M.; Daniels, A. D.; Kudin, K. N.; Strain, M. C.; Farkas, O.; Tomasi, J.; Barone, V.; Cossi,

M.; Cammi, R.; Mennucci, B.; Pomelli, C.; Adamo, C.; Clifford, S.; Ochterski, J.; Petersson, G. A.; Ayala, P. Y.; Cui, Q.; Morokuma, K.; Salvador, P.; Dannenberg, J. J.; Malick, D. K.; Rabuck, A. D.; Raghavachari, K.; Foresman, J. B.; Cioslowski, J.; Ortiz, J. V.; Baboul, A. G.; Stefanov, B. B.; Liu, G.; Liashenko, A.; Piskorz, P.; Komaromi, I.; Gomperts, R.; Martin, R. L.; Fox, D. J.; Keith, T.; Al-Laham, M. A.; Peng, C. Y.; Nanayakkara, A.; Challacombe, M.; Gill, P. M. W.; Johnson, B.; Chen, W.; Wong, M. W.; Andres, J. L.; Gonzalez, C.; Head-Gordon, M.; Replogle, E. S.; Pople, J. A. *Gaussian 98*, revision A.11; Gaussian, Inc.: Pittsburgh, PA, 2001.

(22) Mingdan, C.; Minghong, L.; Jianwen, L.; Yucai, J.; Qianer, Z. *Huaxue Wuli Xuebao* **2002**, *15* (5), 357−362.

(23) Chen, M. D.; Liu, M. L.; Liu, J. W.; Zhang, Q. E.; Au, C. *THEOCHEM* **2002**, 582.

(24) *NIST-JANAF Themochemical Tables*, 4th ed.; Chase, M. W., Ed.; NIST/ACS/APS: 1998; p 647.

(25) Kroto, H. W.; Heath, J. R.; O'Brien, S. C.; Curl, R. F.; Smalley, R. E. *Nature* **1985**, *318*, 162.

(26) Smalley, R. E. *Acc. Chem. Res.* **1992**, *25*, 98.

(27) Alexandrov, A. L.; Schweigert, V. A. *Chem. Phys. Lett.* **1996**, *263*, 551.

(28) von Helden, G.; Hsu, M. T.; Gotts, N. G.; Kemper, P. R.; Bowers, M. T. *Chem. Phys. Lett.* **1993**, *204*, 15.

(29) von Helden, G.; Hsu, M. T.; Gotts, N. G.; Bowers, M. T. *J. Phys. Chem.* **1993**, *97*, 8182.

(30) Bowers, M. T.; Kemper, P.; von Helden, G.; van Koppen, P. *Science* **1993**, *260*, 1446.